Eur Biophys J (1997) 26: 239–245

ARTICLE

F. Gaudin · D. Genest · G. Lancelot

Internal dynamics of d(CGCAAATTTGCG)$_2$: a comparison of NMR relaxation measurements with a molecular dynamics simulation

Received: 19 November 1996 / Accepted: 17 March 1997

Abstract We report the analysis of a 250 ps molecular dynamics simulation of the dodecamer d(CGCAAATTTGCG)$_2$ immersed in a rectangular box of 3469 water molecules with 22 Na$^+$ counterions. The internal dynamics of the molecule were investigated by studying the relevant autocorrelation functions related to the ^{13}C-NMR relaxation parameters of the C1′-H1′ bonds of the sugar rings. The calculated effective correlation times τ_e (~13 ps) and the order parameter S^2 (~0.82) of the Lipari and Szabo formalism (Lipari and Szabo 1982a, b) are in satisfactory agreement with those determined previously by NMR (Gaudin et al. 1995, 1996). ^{1}H-^{1}H NOE buildups have also been measured experimentally and agree with those computed from the simulation. These results validate the simulation, and a more detailed analysis of the internal dynamics of the dodecamer was undertaken. Analysis of the distributions and of the autocorrelation functions of the glycosidic angle flucuations χ shows that the rotational motion of the sugar rings about their glycosidic bond conforms to a restricted diffusion mechanism. The amplitude of the motions and the diffusion constant are 20° and 17.10^9 rad^{2}s^{-1} respectively. These values are in good agreement with ^{13}C NMR data. Furthermore the simulation allows us to rule out another model also consistent with the experiment, consisting of a two-state jump between a syn and an anti conformation.

Key words Molecular dynamics · DNA · NMR relaxation · Correlation times

Introduction

DNA is a semiflexible macromolecule and owing to its length it exhibits complex dynamic behaviour. Its local internal motions have become the subject of increasing interest in recent years. Fast fluctuations in the conformation of DNA may play an important role in transcription and the DNA-protein recognition process. Recent methodological advances in NMR spectroscopy allow one to investigate the internal dynamics of DNA using relaxation measurements (Peng and Wagner 1992; Kay et al. 1992). A limited set of relaxation parameters, typically ^{13}C T$_1$, T$_{1\rho}$ relaxation rates and ^{1}H-^{13}C cross-relaxation rates (NOEs) could characterize the extent of fast internal motions (ps to ns). The interpretation of relaxation data is generally carried out using the "model-free" approach introduced by Lipari and Szabo (1982a, b) which provides information about the spatial restriction of the C-H vector orientation (generalized order parameter: S^2), the effective correlation time of the internal motion (τ_e: ps to ns time scale) and the rotational tumbling motion (τ_g: ns time scale), but not on the true nature of the motions. For the interpretation of NMR relaxation, several simple dynamic models have been reported, such as the rotation diffusion model or the N-site-jump model (Wittebort and Szabo 1978). However, NMR does not provide an accurate description of the motions and therefore relaxation data alone are not sufficient to judge the adequacy of the dynamic models. In contrast, Molecular Dynamics simulation (MD) describes the unaveraged internal motion in the time scale of ps to ns and provide a means of analysing motions at the atomic level and of obtaining a physical description of DNA behaviour. The goal of the present investigation is to use MD to obtain a more complete interpretation of the experimental results and the experimental results to validate the MD procedures.

We have recently studied the extent of the mobility of the C1′-H1′ vector in d(CGCAAATTTGCG)$_2$ by measuring T$_1$ and T$_{1\rho}$ ^{13}C relaxation rates and ^{1}H-^{13}C cross-relaxation rates. Experimental data were in this case interpreted using the Lipari-Szabo approach. Moreover, two dynamic models were used to interpret the NMR relaxation measurements more accurately. A two-state jump model between the anti- and syn-conformations with P(anti)/P(syn) = 91/9 or a restricted rotation about the glycosidic bond model with $D_\chi = \pm 28°$ and an internal diffusion

---

F. Gaudin · D. Genest (✉) · G. Lancelot
Centre de Biophysique Moléculaire, CNRS, Rue Charles Sadron, F-45071 Orléans Cedex 02, France

coefficient of 30.10^9 rad^{2}s^{-1} (not 30.10^7 rad^{2}s^{-1} as erroneaously printed in the paper of Gaudin et al. (1995)) gave a good fit to the experimental data.

In the present paper, we compare the results of the dynamics of the C1′-H1′ vectors as seen by ^{13}C NMR relaxation measurements with a 250 ps MD stimulation of the same dodecamer immersed in a rectangular box containing 3469 water molecules. We also give a comparison of the theoretical and experimental NOE buildup curves for several cross-peaks which provides a rigourous test of the MD based dynamic models for DNA.

The major purposes of the MD simulation are:

- to quantify order parameters (S^2) and effective correlation times τ_e calculated from the Lipari and Szabo analysis and compare them with experimentally determined values.
- to follow the time evolution of NOE intensities for d(CGCAAATTTGCG)$_2$ and compare the NMR measurements with MS simulations.
- to describe the actual nature of the internal motions governing the ^{13}C relaxation of the C1′ of the sugar ring.

Materials and methods

Computational methods

The simulations were performed using the 37C GROMOS force field (van Gunsteren and Berendsen 1987). In this force field, non-polar protons are not treated explicitly. The solution structure of the dodecamer d(CGCAAATTTGCG) served as the starting structure of the MD simulation. These initial coordinates were obtained from a molecular mechanics calculation based on NMR data using the JUMNA program (Lavery 1988).

We configure the system as the dodecamer duplex with 22 Na$^+$ counterions which were initially positioned at 0.5 nm from the phosphorus atom along the OPO bisector. The NaDNA complex was placed at the center of a rectangular box containing 3469 water molecules, resulting in a total of 10 967 atoms, and boundary periodic conditions were adopted. The SPC (simple point charge) model used for water reproduces the radial distribution and dielectric behavior of pure water reasonably well (Berendsen et al. 1987). This molecular system was used as the starting point for molecular dynamics simulations.

In all MD runs the SHAKE algorithm (Ryckaert et al. 1977) with a relative tolerance of 10^{-4} was used to fix all bond lengths. Non-bonded interactions were handled by means of a twin-range method (van Gunsteren and Berendsen 1990) using short and long range interaction cut-off radii of 0.8 and 1.2 nm, respectively. A time step of 2 fs was chosen for integrating the equations of motion. In order to minimize errors due to the cut-off, electrostatic interactions were calculated using the neutral charge groups concept, except for PO_4^- groups and Na$^+$ ions which are charged. An initial run of 200 steps of energy minimization with the steepest descent method was applied to the entire system to relieve any clashes of atoms within the DNA. This was followed by two consecutive heating periods consisting of different runs of molecular dynamics at different temperatures from 50 to 300 K in 50 K steps. Each run consists of a 1 ps simulation at a given temperature with reassignment of atomic velocities every 0.1 ps.

During the first heating period, a harmonic atom position-restraining potential energy term was applied to the dodecamer atoms in order to maintain its original conformation and to equilibrate water in the presence of DNA. The force constant of the position-restraining potential energy term was 9000 kJ mol^{-1} nm^{-2}. During the second heating period, all atoms of the solute and of the solvent were allowed to move, but a weak-semi-harmonic constraint potential ($k_H = 21$ kJ mol^{-1} nm^{-2}) for atoms involved in Watson-Crick base pairing was added as proposed by Swaminathan et al. (1991). Clearly the hydrogen and acceptor atoms are free to move without constraints in the limits 0.18 nm and 0.24 nm but the weak restoring potential is applied if the distance gets beyond these limits.

An extra 50 ps MD run of free equilibration was performed at 300 K. The temperature was maintained at 300 ± 5 K by weakly coupling the dodecamer and the water separately to an external temperature bath (Berendsen et al. 1984) with a coupling constant of 0.1 ps. A subsequent MD trajectory of 250 ps was then carried out. During this production period the atomic trajectories for the coordinates and the velocities were stored every 0.05 ps leading to a total of 5000 configurations for the analysis. Overall rotation and translation of the dodecamer were removed from the MD trajectory by fitting each conformation of the DNA to the first one. Plots of temperature and total energy as a function of time were analyzed to ascertain that the stability of the trajectory was within acceptable limits. The coordinates of the nonpolar hydrogen atoms were incorporated into the MD trajectory by a trivial geometry calculation. The C-H bond length was set at 0.1 nm. The simulation was carried out using an INDY Silicon Graphics work station (100 MIPS) and required approximately 900 hours of CPU time. The average internal structural parameters were computed with the program CURVES (Lavery and Sklenar 1988, 1989).

Calculation of S^2 and τ_e from molecular dynamics trajectory

The MD trajectory was used to obtain the time course of the individual C1′-H1′ vectors. This information was then used to determine the rotational correlation function for the C1′-H1′ vector. The normalized autocorrelation function C(t) of a stationary stochastic function A(t) is given by the ensemble average $\langle A(0)\,A(t)\rangle/\langle A^2(0)\rangle$. The dipolar relaxation between two nuclei in solution can be related to the time correlation function C(t) describing the orientation of the interatomic vector between both nuclei (Abragam 1961). In the ‘model-free’ formalism of Lipari and Szabo the correlation function for an isotropically tumbling molecule with uncorrelated overall and internal motions can be written as

$$C(t) = C_{tumbling}(t)\, C_{int}(t) \quad (1)$$

$C_{tumbling}(t)$ is the correlation function of the overall rotational motion of the molecule considered as a rigid body and $C_{int}(t)$ is the correlation function of the internal rotational motion. The overall motion is considered to be isotropic and $C_{tumbling}(t)$ is given by e^{-t/τ_g} where τ_g is the correlation time of the overall motion.

The relevant A(t) function for calculating the correlation function of the internal motion related to NMR relaxation parameters is:

$$A(t) = \frac{4\pi}{5} \sum_{m=-2}^{m=2} Y_{2m}(\theta_{mol}(t)\,\phi_{mol}(t)) \tag{2}$$

Y_{2m} are the second order spherical harmonics. θ_{mol} and ϕ_{mol} describe the orientation of the C-H vector with respect to the molecular frame. $C_{int}(t)$ has been numerically calculated from MD trajectories:

$$C_{int}(k\delta t) = \sum_{i=1}^{N/2} A(i)\,A(i+k) \Bigg/ \sum_{i=1}^{N} A^2(i) \tag{3}$$

N is the number of configurations, k an integer varying from 0 to N/2 and δt the time step between stored configurations. Therefore correlation functions were evaluated between 0 and 125 ps.

In the model-free approach of Lipari and Szabo, the internal motions are described by a generalized order parameter S^2 and an effective correlation time τ_e. The assumption of the theory of Lipari and Szabo is that the internal motion is much faster than the overall reorientation and that the decay of the internal motion is characterized by a single exponential. According to Lipari-Szabo, the expression for the internal correlation function is given by:

$$C_{int}(t) = (1-S^2)\,e^{-t/\tau_e} + S^2 \tag{4}$$

Using the Marquardt algorithm (1963), $C_{int}(t)$ calculated by Eq. (3) may be fitted with Eq. (4) in order to determine S^2 and τ_e.

Calculation of the glycosidic angle from the MD trajectory

We adapted the subroutine DIHANG of GROMOS to calculate the C2-N1-C1′-H1′ dihedral angle for the pyrimidines and the C4-N9-C1′-H1′ dihedral angle for the purines. The values of the glycosidic angle of each residue were calculated for each configuration (procedure based on the IUPAC conformational coordinates, IUPAC 1983). The average glycosidic angle and its rms were calculated for each nucleotide.

Calculation of NOE from MD simulation

The direct computation of the NOE's requires the knowledge of spectral densities J(0), $J(\omega_H)$, $J(2\omega_H)$; ω_H being the proton Larmor frequency, which cannot be obtained from a MD simulation over a few hundred picoseconds. The dodecamer can be modelled by a cylinder with a length of 4.08 nm and a diameter of 2.05 nm. Consequently, the spectral density computation needs to take into account both the polar and azimuthal fluctuations of interproton vectors, as well as its length variation. A solution to this situation was proposed by Withka et al. (1991, 1992) in which ^1H-^1H NOE buildup rates are calculated with effective correlation times that are dependent on orientation and on the anisotropy of the duplex as well as on the extent of internal motion θ. The expression for the effective correlation time of an internuclear vector is:

$$\begin{aligned}\tau_e = {} & \{1/4 + 9/(8\exp[4\theta^2]) + (3\cos[2\beta])/(2\exp[2\theta^2]) \\ & \quad + (9\cos[4\beta])/(8\exp[4\theta^2])\}/(24D_\perp) \\ & + 3\{(1+1/(2\exp[4\theta^2]) - (2\cos[2\beta])/(\exp[2\theta^2]) \\ & \quad + (\exp[-4\theta^2 - 4\zeta^2]\cos[4\beta])/2\}/(16[2D_\perp + 4D_{||}]) \\ & + 3\{(\exp[-4\theta^2] - \exp[-4\theta^2 - 4\zeta^2]\cos[4\beta])\}/ \\ & \quad (8[5D_\perp + D_{||}])\end{aligned} \tag{5}$$

with $D_{||}$ the tumbling diffusion constant about the z axis, $D_\perp$ the tumbling diffusion constant perpendicular to the z axis, β the angle between the internuclear vector and the z axis, θ^2 the root-mean-square polar angle of motion and ζ^2 the root-mean-square azimuthal angle of motion. The MD trajectories were used to obtain the average values of β, the value of θ from the fluctuation in β and the ζ value from the azimuthal angle fluctuation. The actual value of $D_{||}/D_\perp$ for a double-stranded DNA is not accurately known. The calculations below used $D_{||}/D_\perp = 2.2$ as previously (Gaudin et al. 1995), which was deduced from Tirado and Garcia de la Torre (1979, 1980). The value of $D_\perp$ is equivalent to 1/6 $\tau_\perp$ in which $\tau_\perp$, representing the overall correlation time perpendicular to the symmetry axis, was determined to be 4.3 ns (Gaudin et al. 1995). The cross-relaxation σ_{ij} and spin-lattice relaxation rates ρ_{ij} were calculated in terms of the usual transition probabilities W_0^{ij}, W_1^{ij}, W_2^{ij} and on the basis of the average interproton vector distance obtained as $\langle r_{ij}^{-3}\rangle^2$ from the MD trajectory, with the brackets indicating the time-averaged value. The time course of the NOE buildup is then obtained by solving the generalized Bloch equations by numerical integration.

$$\frac{dP}{dt} = -\rho_{ii}P_i - \sum_{j=1}^{n} \sigma_{ij} P_j n_j \tag{6}$$

P_i is equal to the difference in the spin population at time t from the thermal equilibrium value, n_j is equal to the number of equivalent spins in a group.

^1H-^1H NOE buildup NMR experiments

Two dimensional NOE data were obtained with a Bruker AMX-500 spectrometer for mixing times of 50, 150, 300 ms on a 1.5 mM duplex sample of $d(CGCAAATTTGCG)_2$ in 0.1 M NaCl at pH 7 and a temperature of 22 °C. Typically, NOESY spectra were recorded with 1024 complex datapoints in the t2 domain and 512 increment in t1. The cross peak volumes in the dodecamer spectra were calculated with the integration routines of the UXNMR software package on the Bruker Aspect X32 workstation.

Results

Structural analysis

Table 1 gives some parameters of the average structure of the oligonucleotide. For each parameter, only the value averaged over the 24 residues is reported with its rms. For comparison the values corresponding to the A and B canonical forms are also reported. It is observed that, with the exception of the twist, all the parameters favor the B-form. This observation is reinforced if the average twist is calculated over the 10 central base pairs, since in this case a value of 35° is obtained.

Analysis of C1′H1′ bond correlation functions by the Lipari-Szabo model

The rotational correlation functions for internal motions, $C_{int}(t)$ differ slightly in shape from residue to residue. The correlation functions were calculated for all the residues of the two strands. Typical examples are shown in Fig. 1. For the cases of A5 and T9, $C_{int}(t)$ can be described by a plateau value following a fast initial decay. This shape of the correlation function gives good estimates of S^2 as the plateau level ($t=\infty$) of the correlation function. The rapid decay of this correlation function is fitted by one exponential and allows the calculation of the effective correlation time.

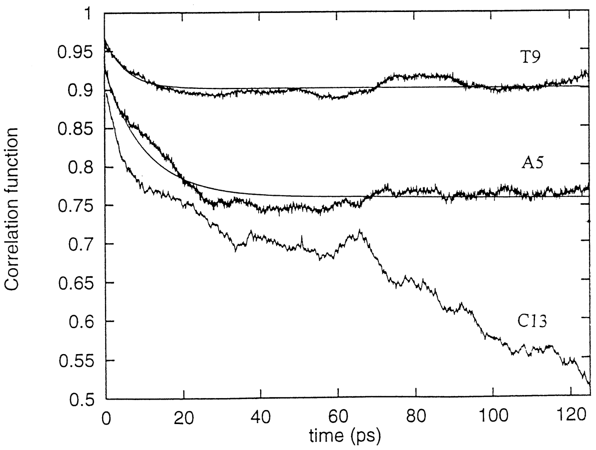

Fig. 1 Correlation functions of the C1′-H1′ vectors of selected nucleotides calculated from MD simulation

Table 1 Example of average structure base pair parameters of the dodecamer d(CGCAAATTTGCG)$_2$. The standard deviations are given in brackets. Angles and distances are given in degrees and Å respectively

	Inclination	Xdis	Twist	Rise	Tilt	Roll
Average	3.03 (9.14)	−1.82 (0.77)	31.07 (12.17)	3.35 (1.07)	2.69 (4.06)	5.78 (8.80)
B form	1.5	−0.70	36.00	3.38	0	0
A form	19.10	−5.40	32.70	2.56	0	0

For 21 out of the 24 C1′-H1′ vectors, the same type of curve as for A5 or T9 was observed, giving rise to well-defined values for S^2 and τ_e. Exceptions are observed for C3, C13 and T20 with no plateau value within the 125 ps of correlation time. For these three residues order parameters and correlation times were not determined. This could either indicate that the plateau value will be reached on a time scale longer than 125 ps or that the reorientation of the C-H bond is too complicated to the described by a rapid motion superimposed on a much slower overall rotational motion. Table 2 gives the values of S^2 and τ_e calculated from MD which are compared to the experimental values obtained previously by NMR (Gaudin et al. 1995). In the experiment, only six residues were selectively ^{13}C-labeled at the C1′ position. Most of the residues have S^2 values in the range 0.8–0.9, indicating that the motions are of relatively small amplitude. Only the two bases at the end were more flexible, characterized by a slight decrease of S^2 ($S^2=0.74$ for C1 and $S^2=0.71$ for G12). The larger fluctuations at the end can be explained by fraying effects. These S^2 values are in reasonable agreement with the experimental ones. The average of S^2 values is 0.80 for NMR and

Table 2 Generalized order parameters and effective correlation time (in ps) from MD (calc) and from NMR (exp) (Gaudin et al. 1995, 1996) for the first strand (*a*) and the second strand (*b*) of the oligonucleotide. S^2_{ave} corresponds to the average of the two strands

	S^2_{cal} (a)	S^2_{cal} (b)	S^2_{ave}	S^2_{exp}	$\tau_{e(cal)}$ (a)	$\tau_{e(cal)}$ (b)	$\tau_{e(ave)}$	$\tau_{e(exp)}$
C	0.74	–	0.74		8	–	8	
G	0.77	0.85	0.81		21	8	14.5	
C	–	0.86	0.86	0.74	–	10	10	31
A	0.96	0.82	0.89	0.79	5	7	6	20
A	0.81	0.79	0.80		11	5	8	
A	0.82	0.75	0.785	0.81	26	24	25	16
T	0.92	0.78	0.85	0.83	7	8	7.5	16
T	0.88	–	0.88	0.83	15	–	15	16
T	0.90	0.78	0.84	0.83	7	11	9	16
G	0.84	0.80	0.82		30	15	22.5	
C	0.86	0.83	0.845		7	12	9.5	
G	0.71	0.73	0.72		20	25	22.5	
Average			0.82	0.80			13.1	19.2

0.82 for MD. Good agreement is also observed for the effective correlation times. The τ_e values from the simulation fluctuate between 5 and 30 ps along the sequence of the dodecamer and the same order of magnitude was found for the experimental values. The average value obtained from MD simulation is 13 ps and is close to the experimental value of 19 ps within experimental accuracy.

Glycosidic distribution

The dihedral glycosidic angles χ distributions were calculated for all the residues of the two strands of the dodecamer. Some examples are given in Fig. 2. The distribution shapes are approximately Gaussian. All glycosidic torsion angles χ are confined to very small conformational regions. The average value which is found for all the residues is close to 250° and is characteristic of B-DNA (258°). Standard deviations are typically 20°, with the exception of the terminal nucleotides, which exhibit a larger amplitude of 25°. As was shown with the S^2 parameters, a greater flexibility is obtained for the residues at the extremities of the dodecamer. The autocorrelation functions of the χ fluctuations have also been calculated (not shown) for each nucleotide of the dodecamer. In all cases they could be fitted by a single exponential with a correlation time τ_χ ranging from 5 to 15 ps.

Because its distribution is Gaussian, the time evolution of χ may be described by a Langevin harmonic oscillator. Among to this model, the restoring torque constant K_χ is $kT/\langle\Delta_\chi^2\rangle$ (k=Boltzman constant, T=absolute temperature and $\langle\Delta_\chi^2\rangle$=mean square fluctuation) and the diffusion constant D_χ is $\langle\Delta_\chi^2\rangle/\tau_\chi$. This leads to approximate values of $3.4 \cdot 10^{-20}$ J rad^{-2} for K_χ and values ranging from $8 \cdot 10^9$ to $25 \cdot 10^9$ rad^{2}s^{-1} for D_χ.

Comparison of ^{1}H-^{1}H NOE buildup rates

The experimental buildup rates of NOE's has been established for a few proton pairs from three NOESY experiments performed at different mixing times. The choice of the proton pairs was based on a sufficiently high signal to noise ratio of the cross peak intensities, on the one hand, and on the absence of overlapping peaks on the other hand. Finally we have looked at intra residue cross peaks corresponding to C3 (H6-H5, H6-H1′ and H6-H2″) and inter residue cross peaks corresponding to the pair G2/C2 (H1′-H6, H2′-H6 and H2″-H6). In the case of the inter

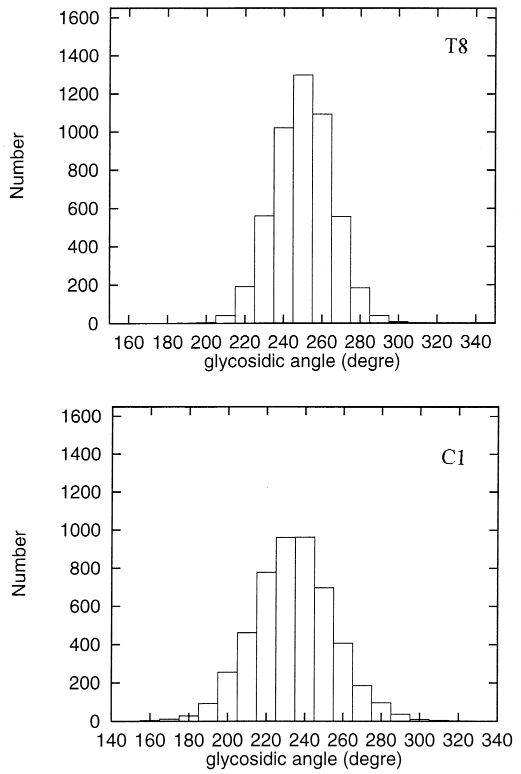

Fig. 2 Distribution of the χ glycosidic angle of the thymine 8 and cytosine 1

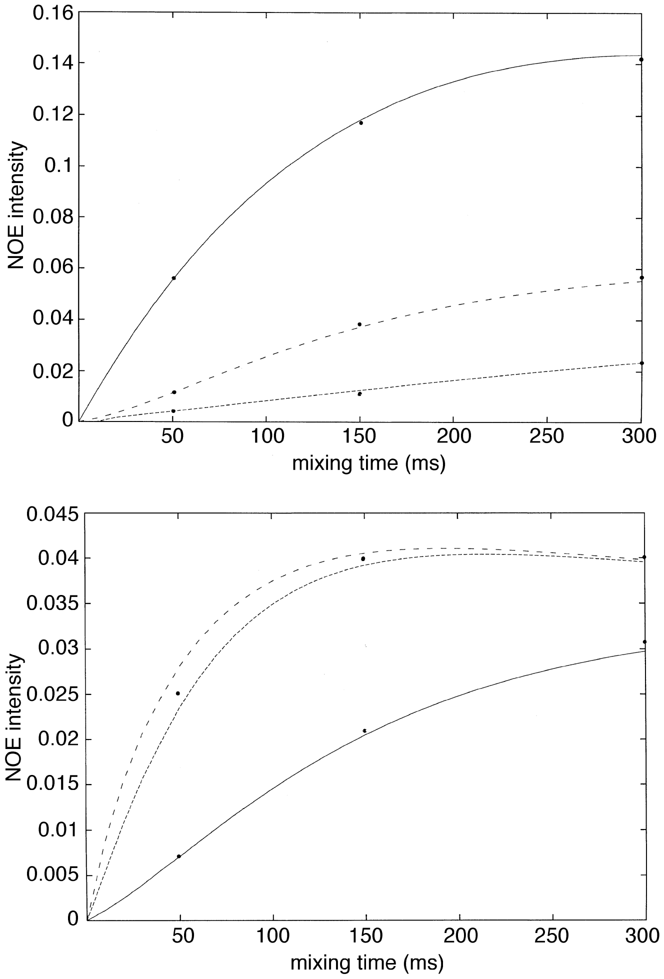

Fig. 3 (*top*) Theoretical (*lines*) and experimental (*points*) NOE buildup curves of the H6 to H1′ (…), H6 to H2″ (---) and H6 to H5 (—) pairs of the cytosine 3; (*bottom*) NOE buildup curves of H1′-H6 (—), H2′-H6 (…) and H2″-H6 (---) pairs of G2-C3

residue cross peaks H2′-H6 and H2″-H6 which overlap, only the average value of their intensities was evaluated. Figure 3 a, b show the comparison between experimental values and values calculated from the MD simulation for the intra residue and inter residue cross peaks respectively. It can be seen that a good agreement is obtained. In particular the simulated intensities corresponding to the inter residues H2′-H6 and H2″-H6 flank the average experimental value.

Discussion and conclusion

The major aim of the present work was to combine information from MD simulation and previously reported experimental NMR data in order to give a more complete picture of the internal motions in DNA. Particular attention has been given to the reorientation motion of the C1′-H1′ bonds to the sugar rings.

The first analysis of the MD trajectory consisted of calculating the relevant internal normalized autocorrelation functions for the orientation of the C1′-H1′ vectors. These functions govern the NMR relaxation process by the intermediate of their Fourier Transform (the so-called spectral densities). The internal correlation functions could be fitted by the sum of a constant term with an exponentially decaying term. On the average the constant is about 0.82, while the average correlation time of the decaying term is 13 ps. Within the limits of experimental accuracy these values are in full agreement with those deduced previously from NMR data (Gaudin et al. 1995) when the model-free analysis of Lipari and Szabo (1982) was used. These values are in agreement with those reported by Koning et al. (1991) and Norberg and Nilsson (1996).

At this point one can ask whether the determination of these parameters can be done from a 250 ps trajectory. It can be noted that each point of the correlation functions was computed using a sampling of 125 ps. The motions we are interested in are characterized by correlation times τ smaller than 25 ps, so that time average is taken over more than 5τ, assuring that ergodicity is a reasonable assumption.

Furthermore, the analysis of some ^{1}H-^{1}H NOE buildup (intra residue and inter residue) shows that the MD simulation satisfactorily reproduces the experimental data. Therefore one can be confident that the simulated dynamics are consistent with different aspects of the experimental relaxation (^{13}C and ^{1}H, T_1 and NOE).

These agreements between the simulation and the experiment encouraged us in the investigation of the actual nature of the internal motions which are responsible for the relaxation of the C1′ spins. In a previous paper, two simple models of the C1′-H1′ motions were considered for interpreting NMR data (Gaudin et al. 1995). Both models assume that the C1′-H1′ internal orientation is only related to the glycosidic torsion angle χ. In the first model a jump between an anti and a syn-conformation was postulated. A good fit between the NMR relaxation parameters deduced from this two-state jump model and the experimental ones was obtained for an equilibrium ratio of the corresponding populations P(anti)/P(syn) = 91/9 and a jump frequency of 10^{11} s^{-1}. In the second model the sugar ring was assumed to rotate about the glycosidic bond according to a restricted diffusion process. In order to account for experimental NMR data, χ was found to fluctuate around 250° within the limits of ±28°, and the diffusion coefficient was $30 \cdot 10^9$ rad^{2}s^{-1}.

NMR data alone could not discriminate between the models. Using the present MD simulation we have determined the distribution function for the χ values of each nucleotide. None of these distributions show the existence of a syn-conformation. Of course this result was obtained from a limited time-scale of 250 ps and it could be argued that on a longer time-scale transitions could be observed. However the sampling of the 24 residues observed during 250 ps can also be considered as the sampling of a unique residue observed during 6 ns. Therefore it seems likely that the two-state jump model can be ruled out.

The analysis of the fluctuations of χ leads to $(\langle\Delta_\chi^2\rangle)^{1/2} = 20°$ and a mean diffusion constant of the order of $17 \cdot 10^9$ rad^{2}s^{-1}. These two values are in reasonably good agreement with those found previously for the restricted diffusion model. Thus it is clear that the present MD simulation allows one to discriminate between the models.

Similar comments can also be made from the analysis of the fluctuations of χ. This angle reflects the rotation about the glycosidic bond of both the sugar ring and the base, assuming they behave as rigid bodies. However, visualization of the internal dynamics shows that the rotational fluctuations of the base are much smaller than those of the sugar ring. Consequently the base motions have little effect on the C1′ relaxation which is mainly governed by the rotation of the sugar ring. The corresponding correlation time is found to be of the order of 10 ps. This analysis can be compared to recent work (Briki and Genest 1996) which shows that the internal motion of the octanucleotide d(CTGATCAG)$_2$ can be well described by translational and rotational motions of rigid sub-units consisting of the bases, the sugar rings and the $PO_4^- + C5'$ groups of atoms. The rotational correlation times for the different sub-units were found to be (7.5 ± 3) ps (Genest 1996), which is in good agreement with the value found for τ_χ in the present study.

Another comparison can be made between the rotation about the glycosidic bond (this work) and the rotation of the bond itself on a plane perpendicular to the axis of the double helix (Briki and Genest 1994), which corresponds to the twist fluctuation. In particular, the restoring torque constant for the twist was of the order of $0.4 \cdot 10^{-18}$ J·rad^{-2}, which is 12 times greater than the restoring torque constant of χ found in the present work. Therefore the potential well for the twist is much more narrow than for χ. Accordingly the angle fluctuations are smaller (about 3 times). The diffusion coefficient for the twist motion was also different (about 25 times smaller). To conclude, these observations allow the following description of the rotational motions of the sugar ring to be given. The transverse motion is characterized by a slow, highly restricted diffusion process whereas the rotation about the glycosidic bond is characterized by a fast and less restricted diffusion process. In conclusion we have shown that Molecular Dynamics simulations can be helpful for interpreting NMR experiments, especially those devoted to the internal dynamics of biomolecules. From NMR alone, it is often difficult to distinguish between different models of motions, and numerical simulations can bring an insight into the actual nature of internal deformations of biopolymers.

References

Abragam A (1961) The principles of nuclear magnetism. Clarendon, Oxford

Berendsen HJC, Postma JPM, van Gunsteren WF, Dinola A, Haak JR (1984) Molecular Dynamics with coupling to an external bath. J Chem Phys 81:3684–3690

Berendsen HJC, Grigera JR, Straatsma TP (1987) The missing term in effective pair potentials. J Chem Phys 91:6269–6271

Briki F, Genest D (1994) Canonical analysis of correlated atomic motions in DNA from molecular dynamics simulation. Bioph Chem 52:35–43

Briki F, Genest D (1995) Molecular dynamics study of the base pair opening process in the self-complementary octanucleotide d(CTGATCAG). J Biomol Struct Dynam 12:1063–1082

Gaudin F, Paquet F, Chanteloup L, Beau JM, Thuong NT, Lancelot G (1995) Selectively ^{13}C-enriched DNA: dynamics of the C1′H1′ vector in d(CGCAAATTTGCG)$_2$. J Biomol NMR 5:49–58

Gaudin F, Chanteloup L, Thuong NT, Lancelot G (1996) Selectively ^{13}C-enriched DNA: Dynamics of the C1′H1′ and C5H5′ or C5′H5″ vectors in d(CGCAAATTTGCG)$_2$. Magn Reson Chem (in press)

Genest D (1996) How long does DNA keep the memory of its conformation? A time-dependent canonical correlation analysis of molecular dynamics simulation. Biopolymers 38:389–399

IUPAC-IUB Joint commission on Biochemical Nomenclature (1983) Eur J Biochem 131:9–15

Kay LE, Nicholson LK, Delaglio F, Bax A, Torchia DA (1992) Pulse sequences for removal of the effects of cross correlation between dipolar and chemical-shift anisotropy relaxation mechanisms on the measurement of heteronuclear T_1 and T_2 values in proteins. J Magn Reson 97:359–375

Koning TMG, Boelens R, van der Marel GA, van Boom JH, Kaptein R (1991) Structure determination of a DNA octamer in solution by NMR spectroscopy. Effect of fast local motions. Biochemistry 30:3787–3797

Lavery R (1988) In: Olson WK, Sarma RH, Sarma MH, Sundaralingam M (eds) Structure and expression, DNA bending and curvature. Adenine Press 3:191–211

Lavery R, Sklenar H (1988) The definition of generalized helical parameters and of axis curvature for irregular nucleic acids. J Biomol Struct Dynam 6:63–91

Lavery R, Sklenar H (1989) Defining the structure of irregular nucleic acids: conventions and principles. J Biomol Struct Dynam 6:655–667

Lipari G, Szabo A (1982a) Model-free approach to the interpretation of nuclear magnetic resonance relaxation in macromolecules. 1. Theory and range of validity. J Am Chem Soc 104:4546–4558

Lipari G, Szabo A (1982b) Model-free approach to the interpretation of nuclear magnetic resonance relaxation in macromolecules. 2. Analysis of experimental results. J Am Chem Soc 104:4559–4570

Marquardt D (1963) An algorithm for least-square estimation of non linear parameters. J Soc Appl Math 11:431–441

Norberg J, Nilsson L (1996) Internal mobility of the oligonucleotide duplexes d(TCGCG)$_2$ and d(CGCGCG)$_2$ in aqueous solution from molecular dynamics simulations. J Biomolecular NMR 7:305–314

Peng JW, Wagner G (1992) Mapping of spectral density functions using heteronuclear NMR relaxation measurements. J Magn Reson 98:308–332

Ryckaert J-P, Ciccotti G, Berendsen HJC (1977) Numerical integration of the cartesian equations of motion of a system with constraints: molecular dynamics of n-alkanes. J Comput Phys 23:327–341

Swaminathan S, Ravishanker G, Beveridge DL (1991) Molecular dynamics of B-DNA including water and counterions: A 140-ps trajectory for d(CGCAAATTTGCG) based on the GROMOS force field. J Am Chem Soc 113:5027–5040

Tirado MM, Garcia de la Torre J (1979) Translational friction coefficients of rigid, symmetric top macromolecules. Application to circular cylinders. J Chem Phys 71:2581–2587

Tirado MM, Garcia de la Torre J (1980) Rotational dynamics of rigid, symmetric top macromolecules. Application to circular cylinders. J Chem Phys 73:1986–1993

Van Gunsteren WF, Berendsen HJC (1987) Groningen Molecular Simulation (GROMOS) Library Manual (Biomos), Nijenborgh 4, 9747 AG Groningen, The Netherlands

Van Gunsteren WF, Berendsen HJC (1990) Computer simulation of molecular dynamics: Methodology, applications, and perspectives in Chemistry. Angew Chem Int Ed Engl 9:992–1023

Wittebort RJ, Szabo A (1978) Theory of NMR relaxation in macromolecules: Restricted diffusion and jump models for multiple internal rotations in amino acid side chains. J Chem Phys 69:1722–1736

Withka JM, Swaminathan S, Beveridge DL, Bolton PH (1991) Time dependence of Nuclear Overhauser Effects of duplex DNA from molecular dynamics trajectories. J Am Chem Soc 113:5041–5049

Withka JM, Swaminathan S, Srinivasan J, Beveridge DL, Bolton PH (1992) Toward a dynamical structure of DNA: comparison of theoretical and experimental NOE intensities. Science 225:597–599

Woessner DE (1962) Nuclear spin relaxation in ellipsoids undergoing rotational brownian motion. J Chem Phys 37:647–654